Chapter 4
Adaptive Biological Networks

Mark D. Fricker, Lynne Boddy, Toshiyuki Nakagaki, and Daniel P. Bebber

Abstract Mycelial fungi and acellular slime molds grow as self-organized networks that explore new territory to search for resources, whilst maintaining an effective internal transport system in the face of continuous attack or random damage. These networks adapt during development by selective reinforcement of major transport routes and recycling of the intervening redundant material to support further extension. In the case of fungi, the predicted transport efficiency of the weighted network is better than evenly weighted networks with the same topology, or standard reference networks. Experimentally, nutrient movement can be mapped using radiotracers and scintillation imaging, and shows more complex transport dynamics, with synchronized oscillations and switching between different pre-existing routes. The significance of such dynamics to the interplay between transport control and topology is not yet known. In a similar manner, the resilience of the network can be tested *in silico* and experimentally using grazing invertebrates. Both approaches suggest that the same structures that confer good transport efficiency also show good resilience, with the persistence of a centrally connected core. The acellular slime mold, *Physarum polycephalum* also forms efficient networks between food sources, with a good balance between total cost, transit distance and fault tolerance. In this case, network formation can be captured by a mathematical model driven by non-linear positive reinforcement of tubes with high flux, and decay of tubes with low flux. We argue that organization of these simple planar networks has been honed by evolution, and they may exemplify potential solutions to real-world compromises between search strategy, transport efficiency, resilience and cost in other domains.

4.1 Introduction

Networks are common within biological systems and have been characterized in a range of different contexts that include metabolism, protein–protein interaction, neural circuits and ecological food webs. Despite the recent progress in biological

M.D. Fricker (✉)
Department of Plant Sciences, University of Oxford, Oxford, OX1 3RB, UK
e-mail: mark.fricker@plants.ox.ac.uk

T. Gross, H. Sayama (eds.), *Adaptive Networks,* Understanding Complex Systems,
DOI 10.1007/978-3-642-01284-6_4, © NECSI Cambridge/Massachusetts 2009

network analysis, one area that has received relatively little attention is the characterization of organisms whose entire growth form is as a network. In particular, both plasmodial slime molds (myxomycetes) and mycelial fungi form elaborate interconnected networks that are highly responsive to local environmental conditions. Unlike the other biological networks described, the network formed by these organisms is not *part* of the organism, it *is* the organism. These networks develop as the organism forages for new resources in a patchy environment and must both transport nutrients between spatially separated source and sink regions, and also maintain their integrity in the face of predation or random damage [4, 5]. The challenges that these conflicting demands place on the network organization have strong parallels with those faced in the design of anthropogenic infrastructure networks. The balance the biological systems have achieved between cost, efficiency and resilience may represent a good compromise to such a combinatorial optimization problem, and may yield useful insights into the design of delocalized, robust infrastructure networks. This presumes that solutions adopted by biological networks will exemplify useful generic theoretical principles, such as persistence, robustness, error-handling or appropriate redundancy, as they have been honed by evolution. The expectation is that the process of Darwinian natural selection based on variation, competition and survival has explored a significant range of possible network organizations and the resulting systems are likely to be well-adapted to survive and reproduce under particular biotic and abiotic conditions to solve certain ecological problems. A range of network architectures, development and dynamics can be found within the fungi and myxomycetes, suggesting a comparative approach may be instructive. However, the constraints imposed by the components used to construct the network (i.e. branching tubes) may have a profound effect on the possible network organization and dynamics, so it is possible that any result can only be generalized to a very limited set of real-world problems.

In this Chapter we focus on recent work describing the structure and function of foraging woodland fungi [3, 33], to illustrate how these essentially planar, weighted spatial networks resolve the conflicting demands of exploration, exploitation, transport and resilience [3]. We provide a brief introduction to network development in Sect. 4.2 then describe predicted transport of such networks in Sect. 4.3 and how it compares with experimentally measured nutrient movement in Sect. 4.4. We further comment on the experimentally observed oscillations and pulsatile transport in Sect. 4.5. Section 4.6 covers both predicted and experimentally determined network robustness. In Sect. 4.7, we compare the results from mycelial fungi with network development in *Physarum*, as a second exemplar of an adaptive biological network, before speculating on the universal features of such biological networks in Sect. 4.8.

4.2 Network Development in Mycelial Fungi

Filamentous fungi grow by apical extension of slender hyphae (Fig. 4.1a) that then branch sub-apically to form a fractal, tree-like mycelium. In ascomycetes and basidiomycetes, tangential hyphal fusions or anastomoses occur as the colony develops to

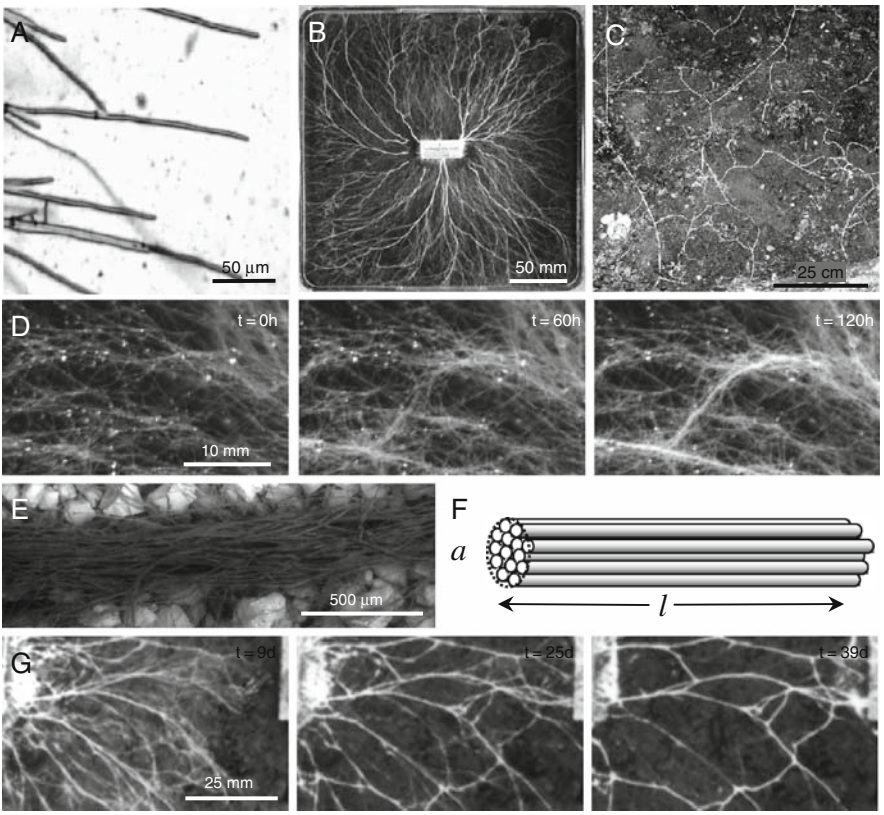

Fig. 4.1 Development of mycelial networks. (**a**) Bright-field image of hyphae of *Phanerochaete velutina* growing across agar. (**b**) Mycelial system of *P. velutina* grown from 4 cm^3 beech wood inocula on a 24 × 24 cm tray of compressed, non-sterile soil after 39 d. (**c**) a 75 × 75 cm portion of an extensive network of the saprotrophic basidiomycete *Megacollybia platyphylla* interconnecting dead wood resources in Wytham Wood, Oxfordshire, UK. (**d**) Time lapse imaging of cord-formation through hyphal aggregation in a growing colony of *P. velutina* on compressed sand/soil. (**e**) Scanning electron micrograph showing the aggregation of hyphae in a cord. (**f**) Schematic representation of a cord illustrating the length (l) and area (a) measures used to weight each link. (**g**) Time lapse imaging of cord-regression and thinning-out of the network in a growing colony of *P. velutina*. Modified from [21]

form an interconnected mycelial network [24, 25, 48, 49]. In the larger, more persistent saprotrophic and ectomycorrhizal basidiomycetes that grow out into soil from colonized food sources, the network architecture develops further with the formation of specialized high-conductivity organs, termed cords or rhizomorphs [12]. These form visible networks interconnecting food resources on a scale of centimetres in laboratory microcosms (Fig. 4.1b) to meters in undisturbed woodland (Fig. 4.1c), through parallel aggregation of many individual hyphae (Fig. 4.1d, e), [18]. Indeed mycelial fungi form the most extensive biological networks so far characterized [16, 33, 52–54], popularly known as the Wood Wide Web [50, 53].

The network topology is defined by classifying junctions (branch-points and anastomoses) as nodes, and the cords between nodes as links. In general, during foraging the number of nodes, number of links and the total material in the network, increase through time. However, the local scale network evolution is also characterized by selective loss of connections and thinning out of the fine mycelium and weaker cords (Fig. 4.1g). This behaviour is also apparent in the box-count mass fractal dimension of these networks, which shows a decrease as the networks thin out [6]. Thus, fungal networks progress from a radial branching tree to a weakly connected lattice-like network behind the growing margin, through a process of fusion and reinforcement to form loops, and selective removal and recycling of excess redundant material [3]. This shift can be quantified by the meshedness or alpha coefficient [11, 26], that gives the number of closed loops or cycles present as a fraction of the maximum possible for a planar network with the same number of nodes. The alpha coefficient measured over the whole colony increased over time from near zero, as expected for a branching tree, to 0.11 ± 0.04 in control systems, and to 0.20 ± 0.05 in systems with an additional wood block resource [3]. The values of the alpha index for *Phanerochaete velutina* were similar to those for networks of tunnels in ant galleries [11], *Physarum polycephalum* (unpublished observations) and street networks in cities [10, 13], suggesting that addition of around 20% of the maximum number of cross-links into a planar network may be sufficient to achieve desirable network properties in a range of different scenarios.

Other topological network measures have not proved to be very informative as they are heavily constrained by the developmental processes of branching and fusion, and crowding effects restricting the maximum number of connections possible in a planar network [2, 3, 3, 19, 29, 33]. Thus, the possible degree (k) of each node is limited to 1 for tips, 3 for branch points or fusion, or occasionally 4 for initially overlapping cords that then fuse. Likewise, the mean clustering coefficient, C [70], is of limited relevance for fungal networks, as their growth habit effectively precludes formation of triads. The frequency distribution of node strength shows more diversity than node degree alone, and follows an approximately log-normal distribution for *P. velutina* networks [3]. However, we have not found evidence for power law relationships that have attracted so much attention in other network analyses.

4.3 Predicted Transport Characteristics of the Mycelial Network

One approach to investigate the transport capacity of the network is to assume that nutrient fluxes will follow the shortest path between pairs of nodes, calculated from the predicted resistance of each link where longer, thinner cords have greater resistance to flow. The changes in thickness of the cords during growth and network re-modeling can be captured by image analysis of the reflected intensity of each cord, with appropriate calibration, to give each link a weight that depends on its length (l) and cross-sectional area (a). Each cord is modeled as a cylinder packed

with identical hyphae (Fig. 4.1f), rather than a single tube that increases in diameter, although the internal structure of cords can be much more complex [62]. An overall measure of transport is the average network efficiency (E), defined as the mean of the reciprocal of shortest path lengths for transport through the network [34, 35].

In isolation, the average efficiency is not useful without some frame of reference. It is not straightforward to generate suitable reference models against which to test the extent that differential cord weighting improves the performance of the network. Indeed elucidation of such biologically-inspired algorithms is a key goal of current research. At present there are no suitable algorithms available to generate weighted planar networks with defined properties. In other areas of network theory, comparisons are typically made with a reference network produced by random rewiring of the links. However, this does not make sense biologically. Likewise, randomly reassigning the weights to different links does not give an intuitively satisfying model to test performance, as it also has no biological basis. We currently use a two stage procedure to evaluate the performance of the fungal networks [3]. In the first step, nodes within the Euclidean fungal network (Fig. 4.2b), were used to construct model networks using well defined neighborhood graphs, including the minimum spanning tree (MST, Fig. 4.2c) as a lower bound giving a low cost, but extremely vulnerable network, the relative neighborhood graph (RNG, Fig. 4.2d), Gabriel graph (GAB, Fig. 4.2e) and the Delaunay triangulation (DT, Fig. 4.2f), giving an upper bound for a well-connected, robust, but rather expensive network [11, 13, 23, 43]. In the second step of analysis, the effect of including a fixed amount of material in the network, equivalent to the total material in the real network (Fig. 4.2a), was examined. Thus, each link in the "uniform" fungal and model networks was allocated a constant weight, such that the total construction cost was the same. Effectively we asked what the consequences for transport would be if the fungus had chosen to allocate the same amount of resource evenly over the existing or model networks, to determine the functional efficiency of the network. This also allowed comparison with the real, differentially weighted network (Fig. 4.2a) as the network measures were in comparable units.

Visual inspection of the resultant networks suggested that the topology of the fungal network had some similarity to the RNG, in terms of the density of cross-linking outside of the inoculum itself (Fig. 4.2d). Quantitatively, the RNGs had an alpha coefficient of $\sim$0.12, slightly lower than the alpha coefficient of the fungal networks. It was also apparent that regression of some links triggered substantial rearrangements in the layout of the model networks, particularly for the MST, which showed dramatic alteration in the connections between neighboring nodes over time (Fig. 4.2c) as the biological network developed.

Perhaps unsurprisingly, the real weighted networks had much shorter physiological paths, especially in the central region, than their corresponding uniform networks [3]. More surprisingly, the weighted fungal network outperformed both the uniform DT and the uniform MST when the predicted transport from just the inoculum to all other nodes was considered (Fig. 4.3). Although very well connected, the DT performed poorly, as distributing material across the large number

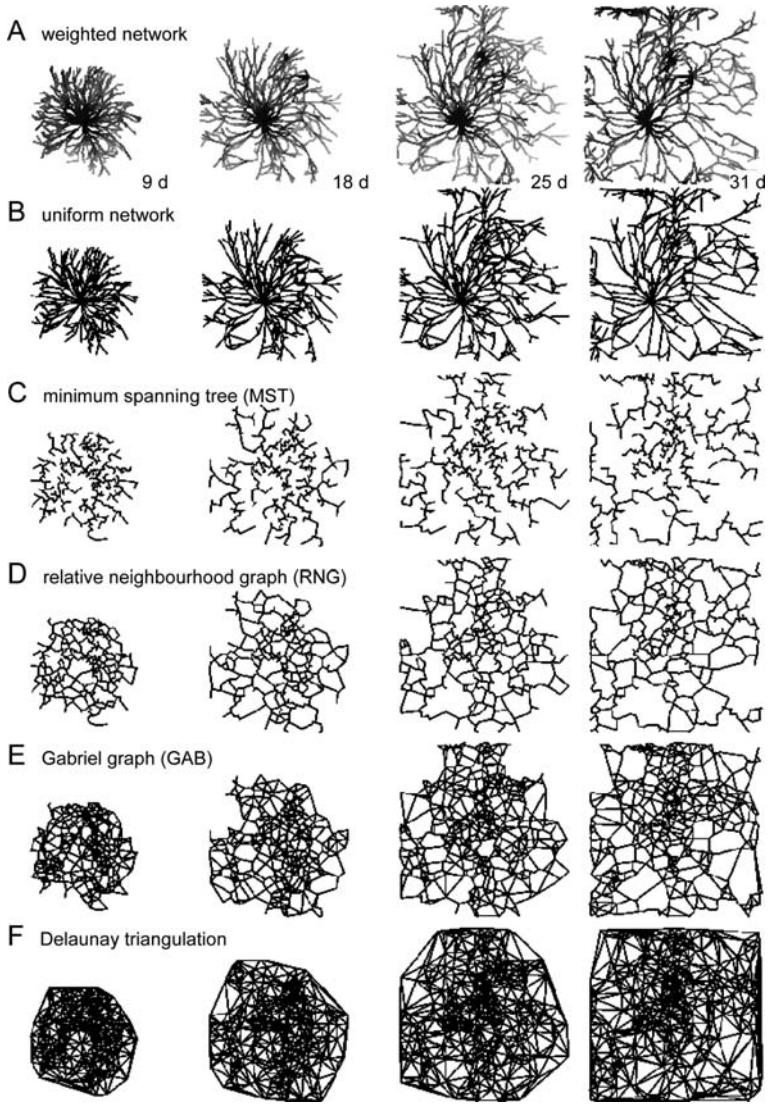

Fig. 4.2 Comparison of weighted fungal networks and neighborhood graphs. *P. velutina* was grown from a wood block inoculum over compressed soil in the presence of an additional wood-block resource, and the weighted network digitized at 9, 18, 25 and 31 d. (**A**) The weighted fungal network, in which line thickness and intensity indicate the relative cross-sectional area of each cord. (**B**) A simplified version of the network that retains nodes arising from branching or fusion, but not nodes simply required to trace the outline of each cord correctly. The amount of material present in the network is distributed evenly across all links to give a uniform network. The nodes present in the simplified graph were then connected according to well-defined rules to give: the minimum spanning tree (**C**); the relative neighborhood graph (**D**); the Gabriel graph (**E**); or the fully connected Delaunay triangulation (**F**). Modified from [21]

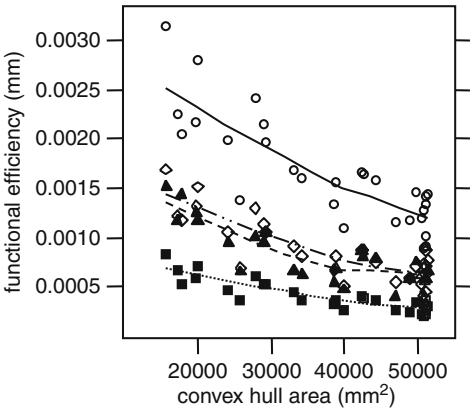

Fig. 4.3 Comparison of transport efficiency between weighted fungal and uniform model networks. The functional efficiency of the fungal network was predicted from the sum of the inverse of the shortest paths from the inoculum to every node as the colony increased in area. The weighted fungal network (○, —) has the highest functional efficiency, in comparison to uniform networks constructed with the same topology (◇, · — · · —), or connected using a Delaunay Triangulation (■, · · ·), or Minimum Spanning Tree (▲, ——). Redrawn from [3]

of links present gave each one low cross-sectional area and consequent high resistance. Conversely, the MST performed better than the DT as it was populated with few, but extremely thick, links. The uniform fungal networks were similar in performance to the MST, although they clearly have a different architecture, but the real weighted fungal network showed the best predicted transport behavior (Fig. 4.3). By normalizing to the DT, the local efficiency (E_{loc}) of the real network, uniform network and MST were calculated as 4.4 ± 0.11, 2.22 ± 0.07 and 2.08 ± 0.12, respectively [3]. Thus, differential weighting of links in the real network gave a > 4 fold improvement in local efficiency in comparison to a fully connected uniform network constructed with the same total cost. The ability of fungal networks to modify link strengths in a dynamic way is, therefore, crucial to achieve high transport capacity.

Subtle shifts in the predicted transport performance of the network as it grows can be identified by which links carry the greatest number of shortest paths and therefore have a high shortest-path betweenness centrality (SPBC) [17, 36]. The relative importance of particular links between the inoculum and added resource, as judged by their SPBC, fluctuate in the early stage of growth with several cords competing before one thickens up sufficiently to achieve dominance [21]. Equally, one of the disadvantages of using shortest path analysis is that comparable parallel pathways that are only marginally longer do not feature prominently in the analysis, but might be expected to participate in transport in a real system. A key area for future development will be to evaluate comparable parallel flow centrality measures.

4.4 Comparison Between Predicted Transport and Experimental Transport

In parallel to the theoretical network analysis, we have developed methods to image nutrient movement directly in these microcosms by mapping the distribution of the amino-acid analogue, ^{14}C-amino isobutyrate (^{14}C-AIB), using photon-counting scintillation imaging (PCSI), [22, 63–66]. ^{14}C-AIB accumulates in the free amino acid pool and is not metabolized in a range of woodland fungi so far examined, as judged by the lack of incorporation of ^{14}C in other metabolites or released as $^{14}CO_2$ [15, 31, 37, 46, 47, 69]. This allows it to be used as a proxy for nitrogen translocation [69] and provides an opportunity to compare the predictions made by the theoretical network analysis to the actual pattern of nutrient movement in the same microcosms [20].

Networks were allowed to develop in microcosms for ~45 d (Fig. 4.4a) and the weighted network digitised (Fig. 4.4b) and analysed to give the link evolution (Fig. 4.4c) and the SPBC (Fig. 4.4d). ^{14}C-AIB was added at the end of the growth period and imaged using photon-counting scintillation imaging (PCSI) to map nutrient movement (Fig. 4.4e). The topological network was then superimposed on the ^{14}C-AIB image to determine the amount of AIB present in each link from the integrated ^{14}C-AIB intensity (Fig. 4.4f). Ideally we would like to calculate the total flux through each link rather than just the integrated amount using knowledge of the amount of ^{14}C-AIB appearing further downstream. However, this is challenging as it requires assumptions about the flow pathway to reallocate the AIB signal correctly. Nevertheless, as a first approximation we have compared ^{14}C-AIB maps with various network parameters such as final link weight (Fig. 4.4g), link evolution (Fig. 4.4h), based on linear regression of the change in link weight with time, and SPBC (Fig. 4.4i). A number of different populations of links were identified. The most prominent were a cluster with high ^{14}C-AIB but low SPBC, corresponding to the tips where the ^{14}C-AIB accumulated. For the other links there was some degree of correlation between the AIB distribution and the network parameter. Equally, the AIB pattern did not always match expectations. For example, there was no obvious reason from the weighted network image why there should be substantial accumulation on the right-hand side of the colony, or little apparent transport to the added resource or beyond (Fig. 4.4e) based on the final link weight (Fig. 4.4b, final panel), link evolution (Fig. 4.4c) or SPBC (Fig. 4.4d). There are clearly additional features governing the control of nutrient distribution that cannot be captured by simple predictions of flow, based solely on network measures or shortest path calculations.

4.5 Oscillations and Pulsatile Transport

In addition to the evolution of the longer term trends described above, a strong pulsatile component was also associated with ^{14}C-AIB transport [22, 64–66]. To characterize this oscillatory behavior, we have analyzed the image-series in the frequency domain and mapped the frequency, phase or magnitude, on a pixel-by-pixel basis as the hue in pseudo-color coded images [22, 64–66]. In single juvenile

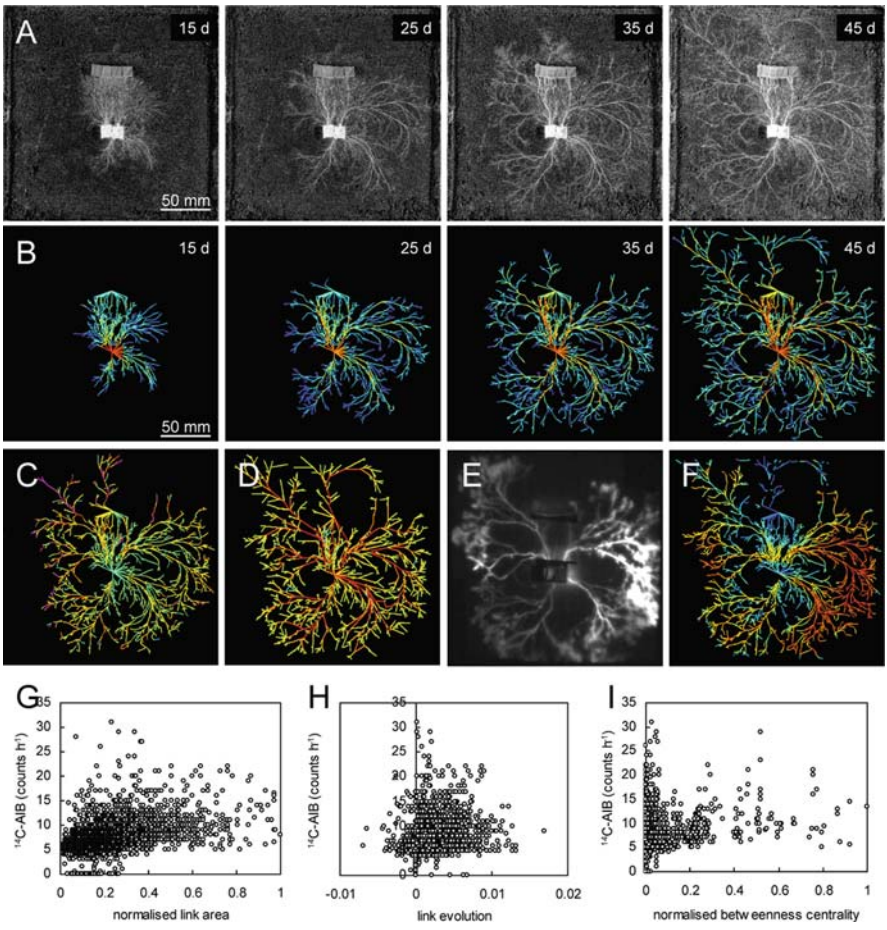

Fig. 4.4 Bright-field images of *P. velutina* growing from a beech wood block inoculum to a set of additional resource wood blocks over compressed soil were obtained at ~3 d intervals for 45 d (**a**). Branch points and anastomoses were manually coded as nodes connected by links, and the cord diameter estimated by image analysis, to give a weighted network (**b**) in which thick cords are represented in red and thin cords in blue, through a rainbow spectrum. Various network parameters were calculated including link evolution (**c**), based on linear regression of the change in link weight with time and color-coded by gradient of the regression equation, and shortest-path betweenness centrality, measured as the number of shortest paths passing through each link (**d**). To compare the predicted transport properties of the network with actual transport, ^{14}C-AIB movement was mapped by photon-counting scintillation imaging (PCSI) at the end of the time-series (**e**) and the amount of AIB present in each link extracted using the digitized network (**f**). The distribution of AIB was then compared with link cross-sectional area at the last time point (**g**), link evolution (**h**) or link betweenness centrality (**i**). Redrawn from [20]

mycelial systems with no additional resource, the mycelium beneath the inoculum and that growing over the screen formed distinct oscillatory domains with the same frequency, but almost 180 degrees out-of-phase with each other [22, 64]. When two colonies were allowed to grow and fuse, the oscillations synchronized between the

two connected inocula but still showed a phase shift with respect to the rest of the colony [22]. Recently we have examined the phase relationships in more complex systems in which arrays of colonies of both compatible and incompatible strains were allowed to grow and fuse. A subset of inocula were labeled and rapid, long-distance transport of ^{14}C-AIB occurred between the connected compatible inocula following fusion, with eventual distribution throughout the super-organism formed

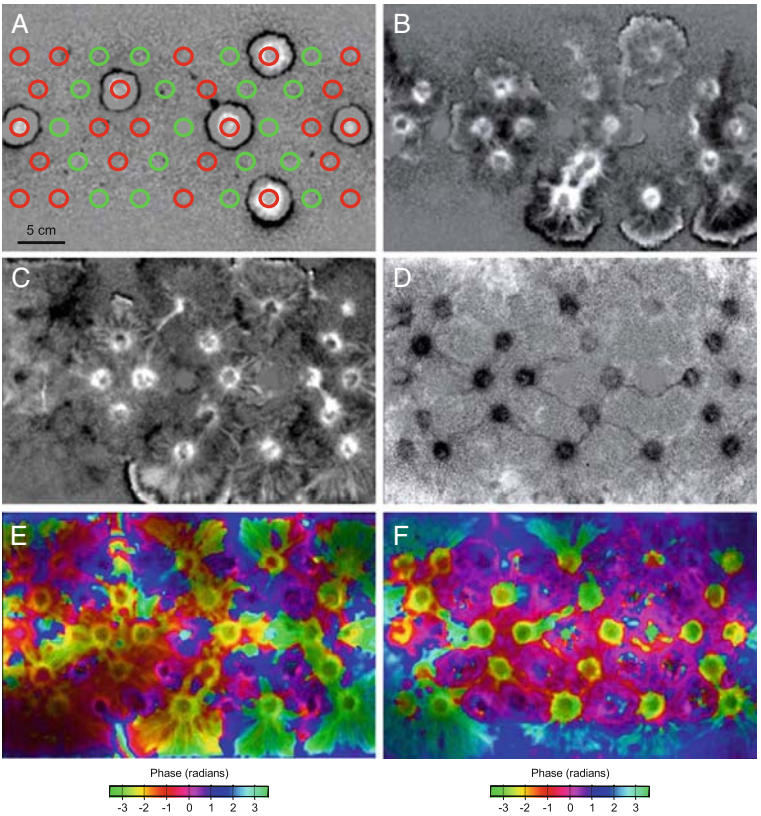

Fig. 4.5 Synchronized oscillations and phase domains in coupled networks. A 9 × 5 array of inocula from two incompatible isolates of *Coniophora puteana* (shown as *red* and *green circles* in panel (**a**) was set up on a scintillation screen. Several inocula were labeled with ^{14}C-AIB and transport imaged using photon-counting scintillation imaging (PCSI) for 12 d. When compatible growing colonies met, they fused and allowed rapid distribution of ^{14}C-AIB throughout the newly inter-connected system. Initially signals from the inoculum and growing mycelium of each colony showed out-of-phase oscillations, which are shown in (**b–d**) as a difference in intensity following subtraction of the long term trend during Fourier analysis. The phase of the oscillations determined from the Fourier analysis on a pixel-by-pixel basis was color-coded (**e** and **f**), in which regions of the same color are oscillating in phase. Before the network was fully connected there was considerable variation in the phase relations across the system (**e**). Following fusion, three domains of synchronized oscillations emerged, that differed in phase (**f**). Thus the interconnected inocula were all synchronized with one phase (*green*), the central domain (*purple*) and the outer, growing margin (*blue*)

(Fig. 4.5a–d). Furthermore, whilst oscillations in the individual colonies were not coupled initially (Fig. 4.5e), they became synchronized following fusion to give a network of linked cords and inocula with one phase, a central mycelial domain within the new super-colony that was phase-shifted by a few hours, and a contiguous foraging margin that was further phase-shifted by a few hours again (Fig. 4.5f). At this stage we do not know what significance to attribute to these oscillating phenomena.

4.6 Network Robustness

High transport capacity and low construction cost could have come at the expense of other network properties, such as robustness to damage, as there is no a priori reason why link weight allocation for one feature necessarily enhances another. This is clearly seen in the improved global transport efficiency of the uniformly weighted MST, even though the MST would be expected to be very vulnerable to disconnection during attack. Robustness to damage, e.g. by physical breakage or grazing by invertebrates [5, 7, 27, 30, 67, 68, 71], is of major significance to long-lived mycelial systems. Having a large number of alternate pathways is important in this context, and the differential strengthening of links not only imparts high transport capacity but also robustness to damage. This can be seen by examining the effects of breaking links in models of the fungal networks in comparison to corresponding uniform networks. We chose to look at link breakage rather than node removal, which is commonly used in other networks, as the cord is the biologically relevant target for attack. Links were broken in order, assuming that the probability of breakage increased with length and decreased with the thickness of the link. That is long, thin links were broken before short, thick ones. Robustness was quantified as the proportion of the total material cost of the network that remained connected to the inoculum. The fungal networks maintained a much greater system connected with the inoculum than did the uniform fungal, DT or MST networks (Fig. 4.6), i.e. the fungal networks were much more robust to damage.

This represents a minimum estimate of the real network resilience in nature, as the network is also able to respond to local damage, by modification of adjacent link strength, and to regrow and reconnect. Thus, for example, local mechanical damage to a small region of the network promoted strengthening of distal circumferential connections (Fig. 4.7a, c). Continuous grazing trimmed the network back to the reinforced core, in support of the *in silico* predictions (Fig. 4.7b), but also promoted an increase in tangential connections (Fig. 4.7d).

4.7 Simple Networks in the Plasmodial Slime Mould *Physarum Polycephalum*

Whilst network analysis of mycelial fungi is in its infancy, considerable progress has already been made in the analysis of simple networks in the plasmodial slime

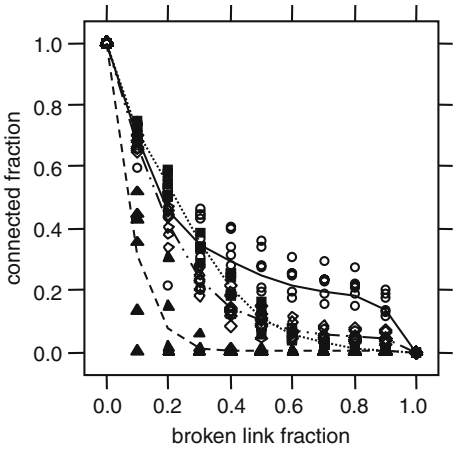

Fig. 4.6 Comparison of network resilience between weighted fungal and uniform model networks. The amount of mycelium remaining connected to the inoculum was measured as an increasing fraction of links were broken. When more than ∼0.3 of the total fraction of the link area was broken, the weighted fungal networks (○, −) maintained a greater connected core than the uniform fungal network (◇, · — · · —), or networks connected using a Delaunay Triangulation (■, · · ·), or Minimum Spanning Tree (▲, ——). Redrawn from [3]

mould *Physarum polycephalum* [32, 38–45, 57–61]. *P. polycephalum* is a large, single-celled amoeboid organism that forages for food resources in a woodland environment. During exploration, it spreads with a relatively contiguous foraging margin to maximize the area searched. However, behind the margin, it resolves this dense structure into a tubular network, interconnecting captured food resources and acting as a supply network to support further exploration.

This natural capacity to construct a transport network can be exploited in experimental microcosms in which food sources (FSs), typically oat flakes, are arranged in specific geometric patterns [39]. As the plasmodium grows, it links each FS encountered in an efficient manner to form a network that includes both direct connections, Steiner points and some additional cross-links that improve both transport efficiency and resilience (Fig. 4.8) [41, 43]. In all cases, the network that is established by the plasmodium has a relatively short total length of interconnecting tubes, but maintains close connections among all the food sources and exhibits a high tolerance to accidental fragmentation.

Growth can also be constrained by physical barriers [44] or influenced by the light regime [40], increasing the opportunity for experimental manipulation to mimic real-world network problems. Thus, for example, *P. polycephalum* can find the shortest path through a maze [40, 44, 45], or connect different arrays of FSs in an efficient manner. For three or more FRs up to about 10, the system strikes a balance between a low total length (TL) of the interconnected network whilst keeping a short connection distance (CD) between any pair of FSs and a high degree of fault tolerance (FT) against accidental disconnection of any tube [41, 43].

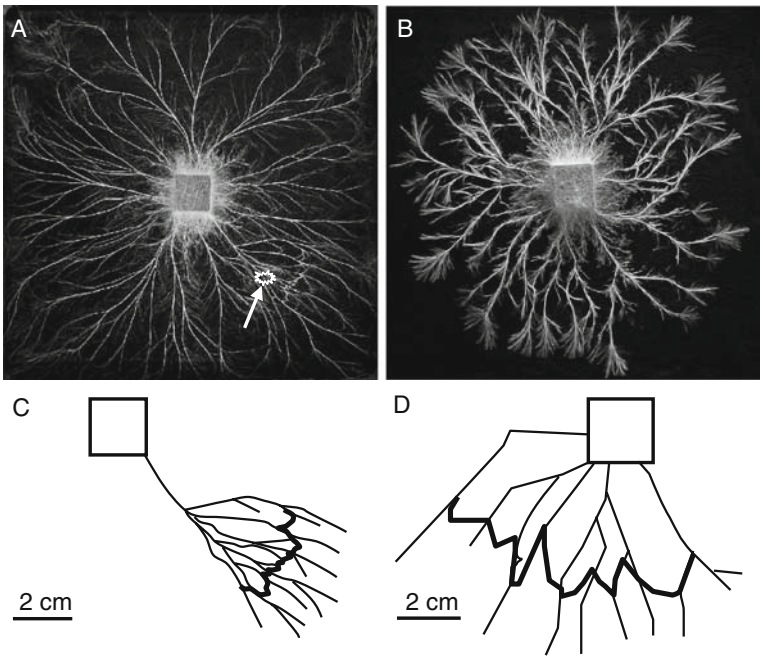

Fig. 4.7 Adaptive network resilience. Colonies of *P. velutina* were grown from 2 × 2 × 2 beech wood blocks over compressed soil in the absence (**a**) or presence (**b**) of grazing by *Folsomia candida*. In (**a**) a localized region of physical damage (indicated by the *arrow*) stimulated a localized increase in tangential connections (**c**). In (**b**) grazing continuously trimmed the finest hyphae, stimulating more local sprouting, and accentuated growth both of the dominant radial cords and also tangential connections (**d**). Redrawn from [19]

The degree of separation is defined as the number of food sources along the shortest path between two food sources. The average separation (AS) is the degree of separation averaged over all pairs of food sources, and decreases as food sources are more closely coupled. To allow comparisons between different arrangements, AS is normalized to the average separation for the minimum spanning tree [41]. The fault tolerance (FT) is the probability that the organism is not fragmented into separate pieces if an accidental breakage occurs at a random point along the tubes. Since the probability of disconnection of a tube is proportional to its length, a longer tube has a higher risk of disconnection. The combined index, FT/TL, can be regarded as a measure of the ratio of benefit to cost. By judicious positioning of food sources, the geometry of the network can be compared to possible theoretical solutions in terms of path length and fault tolerance, such as the minimal spanning tree (MST), the Steiner minimal tree (SMT) and a Delaunay triangulation network (DTN) [41]. Examples are given in Fig. 4.8 for the predicted network with 3 food sources (Fig. 4.8d) and experimental results for 3 food sources (Fig. 4.8e–g), 6 and 7 food sources (Fig. 4.8h, i) with the associated analysis of path length and fault

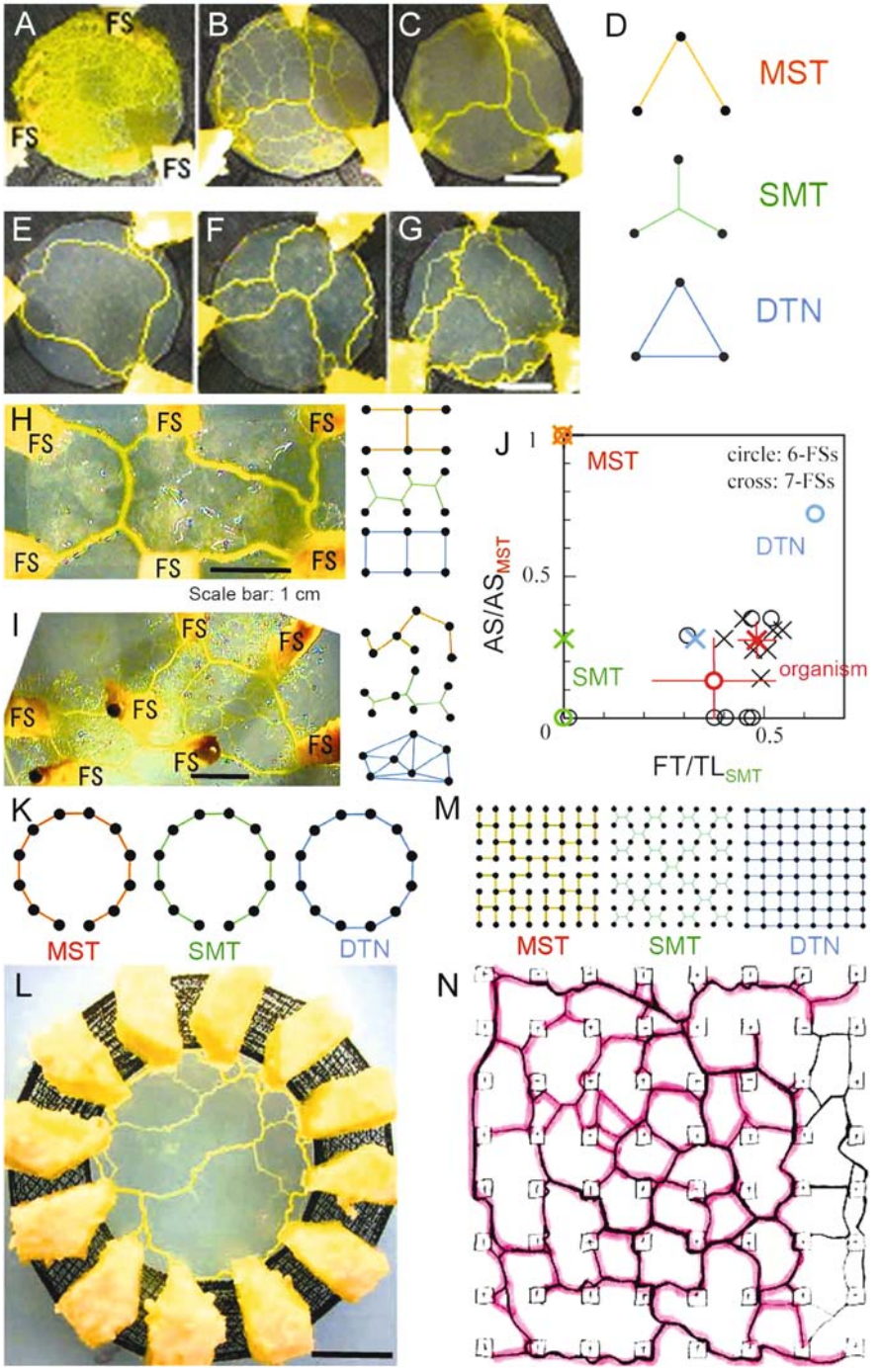

Fig. 4.8 (continued)

tolerance (Fig. 4.8j), rings of 12 food sources (Fig. 4.8k, l) and grids of 64 food sources (Fig. 4.8m, n).

In computational terms, it becomes progressively more challenging to find a good solution to such a combinatorial optimization problem as the number of FSs increases, particularly with the inclusion of Steiner points [61]. It is remarkable, therefore, that solutions reached by *P. polycephalum*, whilst not necessarily optimal individually, cluster around the predicted optimal solution in replicate experiments. Furthermore, the solution is reached rapidly, based only on local information and parallel analogue computing. If it were possible to capture the essence of such a system in simple rules, it might have significant potential to guide de-centralized network development in other domains [39, 42, 58–60].

4.8 Universal Features of Biological Networks?

Characterization of mycelial networks is still in its infancy. However, the network approach provides a way of quantifying and analyzing complex fungal systems for the first time, and also makes it possible to link measurements in microcosms in the laboratory to observations of networks in the field. The simple models predicting transport through such networks, so far based on shortest path considerations through the weighted network, only capture part of the experimentally determined transport behavior. We anticipate that models that include parallel-flow pathways and evolution of the network should improve the match between simulation and experiment, and will benefit from the recent advances in fast algorithms to calculate the necessary metrics. The next conceptual advance will be to identify the rules that allow the network iteratively to refine its structure and transport behavior to yield the network architectures observed. It is conceivable that the identification of such rules will allow development of generic "fungal colony optimization" algorithms

◄

Fig. 4.8 (*Opposite page*) Self-organization of robust network architecture in *Physarum polycephalum*. (a–c) Development of a network between three food sources, starting from a continuous sheet of plasmodium on the surface of agar. Network structure at 0 h (a), 6 h (b) and 36 h (c). Scale bar = 1 cm. (d) Schematic illustration of the arrangement of food sources (*black dots*). The *orange, green* and *blue lines* represent the network of minimum spanning tree (MST), Steiner's minimal tree (SMT) and Delaunay triangulation network (DTN), respectively. (e–g) Three typical networks in ascending order of total length (TL) after 35 h. Scale bar = 1 cm. (h, i) Typical emergent network structure with six (h) and seven (i) food sources (FS) and schematic representation of the corresponding MST (*orange*), SMT (*green*) and DTN (*blue*). (j) Properties of the plasmodial networks, defined by average separation of food sources (AS), normalised to the value for the minimal spanning tree, and benefit to cost ratio, defined as the fault tolerance over the total length (FT/TL). *Black symbols* give the value for each specimen, and *red*, the value of the mean with associated s.e.m. *Orange, green* and *blue symbols* give the values of MST, SMT and DTN respectively. The organism maintains a short total length of tubes with close connections between food sources yet high tolerance of accidental disconnection. (k–n) Network organization with ring (k, l) and grid (m, n) arrangement of food sources. These systems also show robust network architecture, with short path length but high fault tolerance. Redrawn from [43]

similar to those that have evolved from the study of ant colony foraging patterns [14] or based on *P. polycephalum* [40, 41, 58–60].

Even at this stage, some common features of biological network formation seem to emerge. Fungal networks are constructed by local iterative developmental processes rather than predetermined blueprints or centralized control, with growth involving over-production of links and nodes, followed by selective pruning of some links and reinforcement of others. Such a process mimics the process of Darwinian evolution in which natural selection removes less fit offspring. This "Darwinian network model" may be applicable to other biological systems, including foraging ant trails, *P. polycephalum*, axon development and angiogenesis, and may represent a generalized model for growth of physical biological networks. Based on the ant colony and *P. polycephalum* models, we might expect the generic ingredients in such a model will involve a non-linear positive reinforcement term related to the local flux and a linear decay term. Notably this model differs from other models of weighted network evolution that incorporate differential strengthening of links, i.e. "the busiest get busier" [1], rather than differential weakening and loss that is the hallmark of evolution by natural selection. However, the model has parallels with the selective link removal model recently proposed for unweighted networks [51]. In infrastructure networks where costs are associated with creation and maintenance of links, where links differ in some measure of fitness, and where material can be recycled, such a Darwinian model may be applicable. In practical terms such a process may also be witnessed in the evolution of real infrastructure networks, such as British railways following the Beeching reviews in the early '60s [8, 9]. In these reviews, the flux along various routes was measured and routes with too low a level of traffic, mainly branch lines, were targeted for closure. At the same time, major routes were strengthened to cope with the expected source-sink relationships for both passenger and freight traffic. Interestingly, the reports focussed on efficiency rather than any explicit consideration of resilience, which may explain the sensitivity of the current UK rail network to disruption.

A second feature of interest emerging, particularly through consideration of the *P. polycephalum* and fungal networks, is the extent that coupled flows may contain global information. Networks involving physical flows obey continuity equations and are therefore intrinsically coupled across the network. This automatically means that increasing the flow in one part of the network will lead to reductions elsewhere, even though the local conditions in the distal region remain the same. Thus each part of the network is influenced by and can influence the whole network, but without any global assessment of behavior. Useful properties of the network may emerge from the interaction between the local update rules governing topology and flows without the need for long-distance communication or calculation of aggregate properties of the network. It is this coupling in the *P. polycephalum* model that allows the network to resolve from a fine mesh into a quasi-optimal solution [40, 58–60]. Furthermore, the computational overhead for such self-organized networks scales well with the number of additional nodes.

The third general observation on these biological networks is the prevalence of some form of oscillatory process. In *P. polycephalum* it is an actin-myosin contrac-

tion with a short (min) period whilst in the fungal networks it is manifest as a change in the amount of radiolabeled nutrient with a longer (hr to day) period. In both cases the oscillations can synchronize across large regions of the developing system, even if the individual components are asynchronous initially [22, 56, 57]. That the oscillations manage to synchronize is not surprising [55], but the extent that the organisms may be able to interpret and act upon the oscillations is not known. In other contexts, such as supply chains or traffic flow, the existing strategy is to minimize oscillations to achieve maximum throughput [28]. This suggests that either the biological systems lack the additional sensory and feedback systems to suppress oscillations, or that maintaining an oscillatory system is an alternative means to achieve a stable long-term quasi-optimal solution, potentially with less control infrastructure. In *P. polycephalum*, oscillations drive protoplasmic shuttle streaming and generate flows considerably greater than the volume needed simply for extension growth at the margin. It seems likely therefore that the additional energy demands of rhythmic contraction represent the cost of this indirect information transfer. Nevertheless, such a cost is minimal compared to the developmental and behavioral complexity and metabolic cost of the more sophisticated neuron-based sensory systems used by higher organisms.

Acknowledgements Research has been supported by BBSRC (43/P19284), EPSRC (GR/S63090/01), NERC (GR3/12946 and NER/A/S/2002/882), EU Framework 6 (STREP No. 12999), Oxford University Research Infrastructure Fund and the University Dunston Bequest. We thank A. Ashford, K. Burton, P.R. Darrah, D.P. Donnelly, D. Eastwood, J. Efstathiou, J. Hynes, N. Johnson, F. Reed-Tsochas, M. Tlalka, G.M. Tordoff, S.C. Watkinson and members of CABDyN for stimulating discussions.

References

1. Barrat, A., Barthelemy, M., Vespignani, A.: Modeling the evolution of weighted networks. Physical Review E **70**, 066149 (2004)
2. Barrat, A., Barthelemy, M., Vespignani, A.: The effects of spatial constraints on the evolution of weighted complex networks. Journal of Statistical Mechanics p. P05003 (2005)
3. Bebber, D., Hynes, J., Darrah, P., Boddy, L., Fricker, M.: Biological solutions to transport network design. Proceedings of the Royal Society B **274**, 2307–2315 (2007)
4. Bebber, D., Tlalka, M., Hynes, J., Darrah, P., Ashford, A., Watkinson, S., Boddy, L., Fricker, M.: Imaging complex nutrient dynamics in mycelial networks. In: G. Gadd, S. Watkinson, P. Dyer (eds.) Fungi in the Environment, vol. 25, pp. 3–21. Cambridge University Press, Cambridge (2007)
5. Boddy, L., Jones, T.: Mycelial responses in heterogeneous environments: parallels with macroorganisms. In: G. Gadd, S. Watkinson, P. Dyer (eds.) Fungi in the Environment, vol. 25, pp. 112–158. Cambridge University Press, Cambridge (2007)
6. Boddy, L., Wells, J.M., Culshaw, C., Donnelly, D.P.: Fractal analysis in studies of mycelium in soil. Geoderma **88**, 301–328 (1999)
7. Bretherton, S., Tordoff, G.M., Jones, T.H., Boddy, L.: Compensatory growth of *Phanerochaete velutina* mycelial systems grazed by *Folsomia candida* (collembola). FEMS Microbiology Ecology **58**, 33–40 (2006)
8. British Railways Board: The development of the major railway trunk routes (1965)
9. British Transport Commission: The reshaping of british railways - part 1: report (1963)

10. Buhl, J., Gautrais, J., Reeves, N., Sole, R.V., Valverde, S., Kuntz, P., Theraulaz, G.: Topological patterns in street networks of self-organized urban settlements. European Physical Journal B **49**, 513–522 (2006)
11. Buhl, J., Gautrais, J., Sole, R.V., Kuntz, P., Valverde, S., Deneubourg, J.L., Theraulaz, G.: Efficiency and robustness in ant networks of galleries. European Physical Journal B **42**, 123–129 (2004)
12. Cairney, J.W.G.: Basidiomycete mycelia in forest soils: dimensions, dynamics and roles in nutrient distribution. Mycological Research **109**, 7–20 (2005)
13. Cardillo, A., Scellato, S., Latora, V., Porta, S.: Structural properties of planar graphs of urban street patterns. Physical Review E **73**, 066107 (2006)
14. Dorigo, M., Di Caro, G., Gambardella, L.M.: Ant algorithms for discrete optimization. Artificial Life **5**, 137–172 (1999)
15. Elliott, M.L., Watkinson, S.C.: The effect of alpha-aminoisobutyric-acid on wood decay and wood spoilage fungi. International Biodeterioration **25**, 355–371 (1989)
16. Ferguson, B.A., Dreisbach, T.A., Parks, C.G., Filip, G.M., Schmitt, C.L.: Coarse-scale population structure of pathogenic *Armillaria* species in a mixed-conifer forest in the blue mountains of northeast oregon. Canadian Journal of Forest Research **33**, 612–623 (2003)
17. Freeman, L.C.: Set of measures of centrality based on betweenness. Sociometry **40**, 35–41 (1977)
18. Fricker, M., Bebber, D., Boddy, L.: Mycelial networks: structure and dynamics. In: L. Boddy, J. Frankland, P. van West (eds.) Ecology of Saprotrophic Basidiomycetes, vol. 28, pp. 3–18. Academic Press, Amsterdam (2008)
19. Fricker, M., Boddy, L., Bebber, D.: Network organisation of mycelial fungi. In: R. Howard, N. Gow (eds.) The Mycota, vol. VIII, pp. 309–330. Springer-Verlag, Berlin (2007)
20. Fricker, M., Lee, J., Bebber, D., Tlalka, M., Hynes, J., Darrah, P., Watkinson, S., Boddy, L.: Imaging complex nutrient dynamics in mycelial networks. Journal of Microscopy **231**, 299–316 (2008)
21. Fricker, M., Lee, J., Boddy, L., Bebber, D.: The interplay between structure and function in fungal networks. Topologica **1**, 004 (2008)
22. Fricker, M.D., Tlalka, M., Bebber, D., Takagi, S., Watkinson, S.C., Darrah, P.R.: Fourier-based spatial mapping of oscillatory phenomena in fungi. Fungal Genetics and Biology **44**, 1077–1084 (2007)
23. Gastner, M.T., Newman, M.E.J.: Shape and efficiency in spatial distribution networks. Journal of Statistical Mechanics p. P01015 (2006)
24. Glass, N.L., Jacobson, D.J., Shiu, P.K.T.: The genetics of hyphal fusion and vegetative incompatibility in filamentous ascomycete fungi. Annual Review of Genetics **34**, 165–186 (2000)
25. Glass, N.L., Rasmussen, C., Roca, M.G., Read, N.D.: Hyphal homing, fusion and mycelial interconnectedness. Trends in Microbiology **12**, 135–141 (2004)
26. Haggett, P., Chorley, R.: Network Analysis in Geography. Arnold, London (1969)
27. Harold, S., Tordoff, G.M., Jones, T.H., Boddy, L.: Mycelial responses of *Hypholoma fasciculare* to collembola grazing: effect of inoculum age, nutrient status and resource quality. Mycological Research **109**, 927–935 (2005)
28. Helbing, D.: Traffic and related self-driven many-particle systems. Reviews of Modern Physics **73**, 1067–1141 (2001)
29. Hitchcock, D., Glasbey, C.A., Ritz, K.: Image analysis of space-filling by networks: application to a fungal mycelium. Biotechnology Techniques **10**, 205–210 (1996)
30. Kampichler, C., Rolschewski, J., Donnelly, D.P., Boddy, L.: Collembolan grazing affects the growth strategy of the cord-forming fungus *Hypholoma fasciculare*. Soil Biology and Biochemistry **36**, 591–599 (2004)
31. Kim, K.W., Roon, R.J.: Transport and metabolic effects of alpha-aminoisobutyric-acid in *Saccharomyces cerevisiae*. Biochimica et Biophysica Acta **719**, 356–362 (1982)
32. Kobayashi, R., Tero, A., Nakagaki, T.: Mathematical model for rhythmic protoplasmic movement in the true slime mold. Journal of Mathematical Biology **53**, 273–286 (2006)

33. Lamour, A., Termorshuizen, A.J., Volker, D., Jeger, M.J.: Network formation by rhizomorphs of *Armillaria lutea* in natural soil: their description and ecological significance. FEMS Microbiology Ecology **62**, 222–232 (2007)
34. Latora, V., Marchiori, M.: Efficient behavior of small-world networks. Physical Review Letters **87**, 198701 (2001)
35. Latora, V., Marchiori, M.: Economic small-world behavior in weighted networks. European Physical Journal B **32**, 249–263 (2003)
36. Latora, V., Marchiori, M.: A measure of centrality based on network efficiency. New Journal of Physics **9**, 188 (2007)
37. Lilly, W.W., Higgins, S.M., Wallweber, G.J.: Uptake and translocation of 2-aminoisobutyric acid by *Schizophyllum commune*. Experimental Mycology **14**, 169–177 (1990)
38. Nakagaki, T.: Smart behavior of true slime mold in a labyrinth. Research in Microbiology **152**, 767–770 (2001)
39. Nakagaki, T., Guy, R.D.: Intelligent behaviors of amoeboid movement based on complex dynamics of soft matter. Soft Matter **4**, 57–67 (2008)
40. Nakagaki, T., Iima, M., Ueda, T., Nishiura, Y., Saigusa, T., Tero, A., Kobayashi, R., Showalter, K.: Minimum-risk path finding by an adaptive amoebal network. Physical Review Letters **99**, 068104 (2007)
41. Nakagaki, T., Kobayashi, R., Nishiura, Y., Ueda, T.: Obtaining multiple separate food sources: behavioural intelligence in the *Physarum* plasmodium. Proceedings of the Royal Society of London Series B **271**, 2305–2310 (2004)
42. Nakagaki, T., Saigusa, T., Tero, A., Kobayashi, R.: Effects of amount of food on path selection in the transport network of an amoeboid organism. In: Proceedings of the International Symposium on Topological Aspects of Critical Systems and Networks. World Scientific (2007)
43. Nakagaki, T., Yamada, H., Hara, M.: Smart network solutions in an amoeboid organism. Biophysical Chemistry **107**, 1–5 (2004)
44. Nakagaki, T., Yamada, H., Toth, A.: Maze-solving by an amoeboid organism. Nature **407**, 470–470 (2000)
45. Nakagaki, T., Yamada, H., Toth, A.: Path finding by tube morphogenesis in an amoeboid organism. Biophysical Chemistry **92**, 47–52 (2001)
46. Ogilvie-Villa, S., Debusk, R.M., Debusk, A.G.: Characterization of 2-aminoisobutyric acid transport in *Neurospora crassa* – a general amino-acid permease-specific substrate. Journal of Bacteriology **147**, 944–948 (1981)
47. Olsson, S., Gray, S.N.: Patterns and dynamics of ^{32}P-phosphate and labelled 2-aminoisobutyric acid (^{14}C-AIB) translocation in intact basidiomycete mycelia. FEMS Microbiology Ecology **26**, 109–120 (1998)
48. Rayner, A., Griffith, G., Ainsworth, A.: Mycelial interconnectedness. In: N. Gow, G. Gadd (eds.) The Growing Fungus, pp. 21–40. Chapman and Hall, London (1994)
49. Rayner, A., Watkins, Z., Beeching, J.: Self-integration - an emerging concept from the fungal mycelium. In: N. Gow, G. Robson, G. Gadd (eds.) The Fungal Colony, pp. 1–24. Cambridge University Press, Cambridge (1999)
50. Read, D.: Mycorrhizal fungi – the ties that bind. Nature **388**, 517–518 (1997)
51. Salathe, M., May, R.M., Bonhoeffer, S.: The evolution of network topology by selective removal. Journal of the Royal Society Interface **2**, 533–536 (2005)
52. Simard, S.W., Durall, D.M.: Mycorrhizal networks: a review of their extent, function, and importance. Canadian Journal of Botany **82**, 1140–1165 (2004)
53. Simard, S.W., Perry, D.A., Jones, M.D., Myrold, D.D., Durall, D.M., Molina, R.: Net transfer of carbon between ectomycorrhizal tree species in the field. Nature **388**, 579–582 (1997)
54. Smith, M.L., Bruhn, J.N., Anderson, J.B.: The fungus *Armillaria bulbosa* is among the largest and oldest living organisms. Nature **356**, 428–431 (1992)
55. Strogatz, S.H.: From kuramoto to crawford: exploring the onset of synchronization in populations of coupled oscillators. Physica D **143**, 1–20 (2000)

56. Takamatsu, A., Tanaka, R., Yamada, H., Nakagaki, T., Fujii, T., Endo, I.: Spatiotemporal symmetry in rings of coupled biological oscillators of *Physarum* plasmodial slime mold. Physical Review Letters **87**, 078102 (2001)
57. Tero, A., Kobayashi, R., Nakagaki, T.: A coupled-oscillator model with a conservation law for the rhythmic amoeboid movements of plasmodial slime molds. Physica D **205**, 125–135 (2005)
58. Tero, A., Kobayashi, R., Nakagaki, T.: Physarum solver: A biologically inspired method of road-network navigation. Physica A **363**, 115–119 (2006)
59. Tero, A., Kobayashi, R., Nakagaki, T.: A mathematical model for adaptive transport network in path finding by true slime mold. Journal of Theoretical Biology **244**, 553–564 (2007)
60. Tero, A., Nakagaki, T., Toyabe, K., Yumili, K., Kobayashi, R.: A method inspired by physarum for solving the steiner problem. International Journal for Unconventional Computing **in press** (2009)
61. Tero, A., Yumiki, K., Kobayashi, R., Saigusa, T., Nakagaki, T.: Flow-network adaptation in physarum amoebae. Theory in Biosciences **127**, 89–94 (2008)
62. Thompson, W., Rayner, A.D.M.: Structure and development of mycelial cord systems of *Phanerochaete laevis* in soil. Transactions of the British Mycological Society **78**, 193–200 (1982)
63. Tlalka, M., Bebber, D., Darrah, P., Watkinson, S., Fricker, M.: Dynamic resource allocation and foraging strategy in mycelial systems. Fungal Genetics and Biology **45**, 1111–1121 (2008)
64. Tlalka, M., Bebber, D., Darrah, P.R., Watkinson, S.C., Fricker, M.D.: Emergence of self-organised oscillatory domains in fungal mycelia. Fungal Genetics and Biology **44**, 1085–1095 (2007)
65. Tlalka, M., Hensman, D., Darrah, P.R., Watkinson, S.C., Fricker, M.D.: Noncircadian oscillations in amino acid transport have complementary profiles in assimilatory and foraging hyphae of *Phanerochaete velutina*. New Phytologist **158**, 325–335 (2003)
66. Tlalka, M., Watkinson, S.C., Darrah, P.R., Fricker, M.D.: Continuous imaging of amino-acid translocation in intact mycelia of *Phanerochaete velutina* reveals rapid, pulsatile fluxes. New Phytologist **153**, 173–184 (2002)
67. Tordoff, G.M., Boddy, L., Jones, T.H.: Grazing by *Folsomia candida* (collembola) differentially affects mycelial morphology of the cord-forming basidiomycetes *Hypholoma fasciculare*, *Phanerochaete velutina* and *Resinicium bicolor*. Mycological Research **110**, 335–345 (2006)
68. Tordoff, G.M., Boddy, L., Jones, T.H.: Species-specific impacts of collembola grazing on fungal foraging ecology. Soil Biology and Biochemistry **40**, 434–442 (2008)
69. Watkinson, S.C.: Inhibition of growth and development of *Serpula lacrimans* by the non-metabolized amino-acid analog alpha-aminoisobutyric-acid. FEMS Microbiology Letters **24**, 247–250 (1984)
70. Watts, D.J., Strogatz, S.H.: Collective dynamics of 'small-world' networks. Nature **393**, 440–442 (1998)
71. Wood, J., Tordoff, G.M., Jones, T.H., Boddy, L.: Reorganization of mycelial networks of *Phanerochaete velutina* in response to new woody resources and collembola (*Folsomia candida*) grazing. Mycological Research **110**, 985–993 (2006)